EurJIC
European Journal of Inorganic Chemistry

Research Article
doi.org/10.1002/ejic.202300267

Chemistry Europe
European Chemical Societies Publishing

www.eurjic.org

Special Collection

Regioselective Rhodium-Catalyzed 1,2-Hydroboration of Pyridines and Quinolines Enabled by the Tris(8-quinolinyl)phosphite Ligand

Miguel A. Chacón-Terán,[a, e] Vanessa R. Landaeta,*[a, b, d] Robert Wolf,*[b] and Rafael E. Rodríguez-Lugo*[b, c, d]

Dedicated to Professor Rainer Streubel on the occasion of his 65th birthday.

A Rh(I) complex [κ^2(*P,N*)-{P(Oquin)$_3$}RhCl(PPh$_3$)] (**1**) bearing the P,N ligand tris(8-quinolinyl)phosphite, P(Oquin)$_3$, has been synthesized and structurally characterized. The molecular structure of complex **1** shows that P(Oquin)$_3$ acts as a bidentate P,N chelate ligand. Reactivity studies of **1** reveal that the triphenylphosphine ligand can be replaced by PCy$_3$ or removed upon oxidation with concomitant coordination of a second 8-quinolyl unit of P(Oquin)$_3$. In addition, the Rh(III) complex [RhCl$_2${OP(Oquin)$_2$}] (**3**), resulting from treating **1** with either wet CDCl$_3$ or, sequentially, with HCl and water, was identified by X-ray diffraction analysis. Complex **1** catalyzes the 1,2-regioselective hydroboration of pyridines and quinolines, affording *N*-boryl-1,2-dihydropyridines (1,2-BDHP) and *N*-boryl-1,2-hydroquinolines (1,2-BDHQ) in high yield (up to >95%) with turnover numbers (TONs) of up to 130. The system tolerates a variety of substrates of different electronic and steric nature. In comparison with other transition-metal-based hydroboration catalysts, this system is efficient at a low catalyst loading without the requirement of base or other additives.

[a] *Dr. M. A. Chacón-Terán, Dr. V. R. Landaeta*
Departamento de Química
Universidad Simón Bolívar
Valle de Sartenejas, Baruta. Apartado 89000, Caracas 1020-A (Venezuela)

[b] *Dr. V. R. Landaeta, Prof. Dr. R. Wolf, Dr. R. E. Rodríguez-Lugo*
Institute of Inorganic Chemistry
University of Regensburg
93040 Regensburg (Germany)
E-mail: vanessa.landaeta@ur.de
robert.wolf@ur.de
rafael-emilio.rodriguez-lugo@ur.de

[c] *Dr. R. E. Rodríguez-Lugo*
Laboratorio de Química Bioinorgánica, Centro de Química
Instituto Venezolano de Investigaciones Científicas (IVIC)
Carretera Panamericana Km. 11, Altos de Pipe Caracas 1020-A (Venezuela)

[d] *Dr. V. R. Landaeta, Dr. R. E. Rodríguez-Lugo*
*Current address:*Istituto di Chimica dei Composti Organometallici
Consiglio Nazionale delle Ricerche
Via Madonna del Piano 10, 50019 Sesto Fiorentino (Italy)

[e] *Dr. M. A. Chacón-Terán*
*Current address:*Department of Chemistry and Biochemistry
University of California, Merced
5200 Lake Rd, Merced, CA 95343 (USA)

[**] *A previous version of this manuscript has been deposited on a preprint server (https://epub.uni-regensburg.de/44257/1/PhD%20Thesis%20Miguel%20Chacon%20USB_UR%20FINAL.pdf).*

Supporting information for this article is available on the WWW under https://doi.org/10.1002/ejic.202300267

Special Collection *Part of the celebratory collection for Rainer Streubel.*

Introduction

Dearomative transformations of pyridine derivatives are of much interest because they can provide access to partially unsaturated cyclic compounds, such as 1,2-dihydropyridine (DHP) and 1,2-dihydroquinoline (DHQ) derivatives, which are useful intermediates for the synthesis of nitrogen-containing organic molecules.[1—7] Known examples of dearomative transformations involve the stoichiometric formation of pyridinium salts,[2—4,8] in which a nucleophilic attack to the pyridine ring is facilitated.[9] Transition metal-catalyzed addition reactions to pyridines constitute an attractive strategy for the reduction of these *N*-heterocyclic rings, which circumvents the stoichiometric activation via pyridinium salts. Although the direct hydrogenation of the nitrogen heterocycles is the simplest pathway to reduce pyridine rings, the harsh reaction conditions required and ensuing overreduction to form piperidine derivatives are often problematic.[10—12] Alternative procedures include catalytic hydrosilylation reactions, which afford silylated di- and tetrahydropyridine derivatives.[13—21] However, most existing hydrosilylation systems are inconvenient in terms of over-reduction,[13,14] low selectivity[18] and narrow substrate scope.[16,22]

In 2011, the group of Suginome found that pyridine derivatives undergo addition of silylboronic esters in the presence of a palladium catalyst to yield *N*-boryl-4-silyl-1,4-dihydropyridines.[23] This was the first example of catalytic addition of non-hydrogen elements onto the carbon atoms of pyridine rings. It was assumed that one of the driving forces of the reaction is the formation of the strong B–N bond. Subsequently, it was envisioned that the use of boron-

Research Article
doi.org/10.1002/ejic.202300267

Chemistry Europe
European Chemical Societies Publishing

containing reagents would promote the addition to pyridine rings. Catalytic hydroboration (HB)[24—27] has therefore been proposed as a feasible alternative to hydrogenation for the dearomative reduction of pyridines.[22,28—40] Marks and co-workers[28] and the group of Ohmura and Suginome[29] described the first early (lanthanide) and late (rhodium) transition-metal-catalyzed hydroboration of pyridines giving *N*-boryl-1,2-hydropyridines in a regioselective manner (see Figure 1). Examples of magnesium-catalyzed hydroboration of pyridine derivatives, either yielding a mixture of 1,2- and 1,4-DHP compounds,[30,41] or the 1,2-isomer selectively (Figure 1),[31] have also been reported in the literature. 1,4-hydroborated products can be selectively obtained using metal catalysts based on K,[32] Ni (Figure 1),[33] Zn,[22] Ge,[40] Zr,[34] Ru (Figure 1),[35] or Ce[36] compounds, cooperative Cu/Fe-heterobimetallic[42] or Ni/Al-heterotrimetallic scaffold[43] or Hf-based metal—organic frameworks,[34] organocatalytic protocols involving either organoboranes[44—48] or organophosphanes,[49,50] or even under basic, catalyst-free conditions.[51,52] By contrast, the 1,2-regioselective reduction of *N*-heteroaromatic compounds is a much more challenging task (Figure 1).[21,28,29,31,37,38,53,54] Of these, the metal-catalyzed systems use catalyst loadings typically of 1—2 mol%,[28,29,31,37,38] require addition of basic ligands[29] or return only moderate yields of product.[37] The development of efficient catalytic methodologies for the selective partial reduction of pyridines and quinolines to 1,2-DHP and 1,2-DHQ derivatives under mild conditions is, therefore, highly desirable, and becomes then an interesting goal.

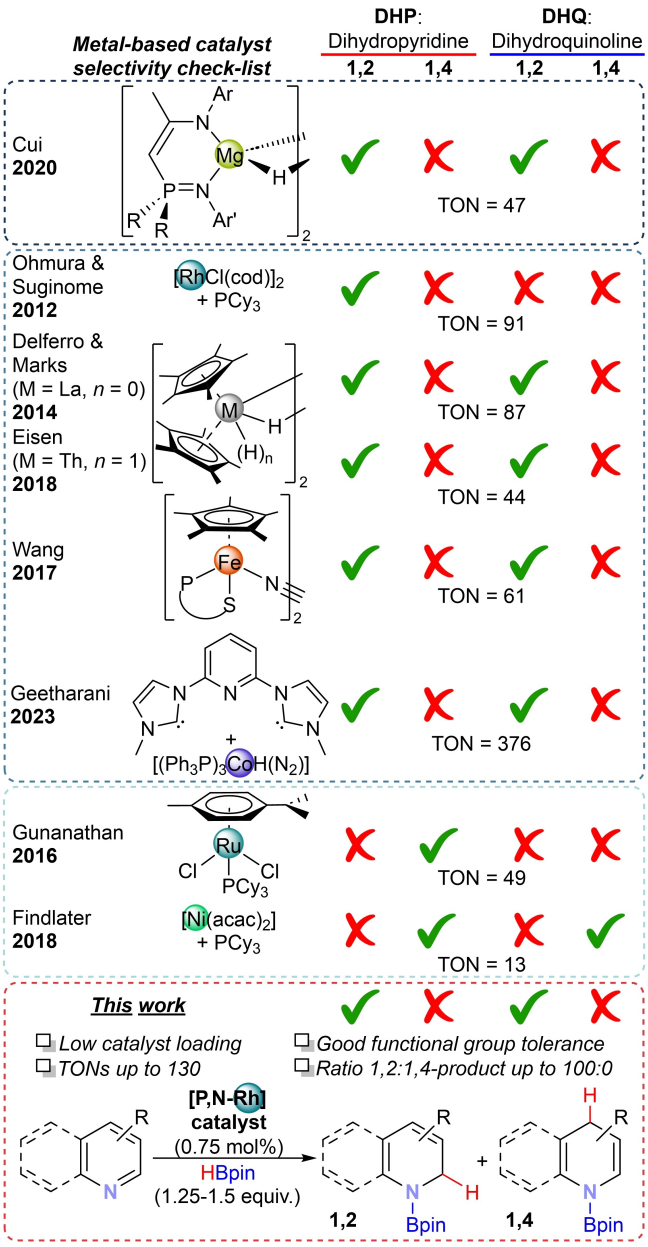

Figure 1. Metal-based methodologies from the literature contrasted with the system herein reported, in the partial reduction of pyridines and quinolines.

In 2018, some of us reported the hybrid phosphite compound tris(8-quinolinyl)phosphite, P(Oquin)$_3$.[55] Our studies have demonstrated the potential of this phosphite ligand in homogeneous-catalyzed oxidation reactions using palladium catalysts[55] and as an organocatalyst in metal-free transfer hydrogenations.[56] The interest in this ligand resides in its variable denticity, and in its combination of both *soft* and *hard* donor atoms on the same ligand scaffold.[57] These characteristics could be useful in the stabilization of transition metal species and could favorably influence the catalytic properties, e.g. through hemilability, as observed for other P,N ligands.[58—60]

Herein, we describe the synthesis, characterization, and reactivity of the rhodium(I) complex [κ^2(*P,N*)-{P(Oquin)$_3$}RhCl(PPh$_3$)] (**1**), and we show that this compound effectively catalyzes the regioselective 1,2-hydroboration of pyridines and quinolines using a catalyst loading of 0.75 mol%.[29,31,37,38,53] Rhodium-based catalysts continue to attract attention in borylation reactions of a variety of substrates.[61]

Results and Discussion

Synthesis and Characterization of the Rh(I) Complex

Our study began with the synthesis of complex [κ^2(*P,N*)-{P(Oquin)$_3$}RhCl(PPh$_3$)] (**1**). The compound is formed according to Scheme 1 by reacting either [(cod)RhCl(PPh$_3$)] (cod = 1,5-cyclooctadiene) or [(PPh$_3$)$_3$RhCl] (Wilkinson's catalyst) with

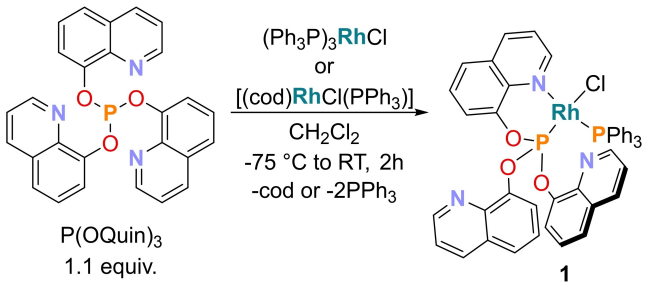

Scheme 1. Synthesis of the rhodium (I) complex [κ^2(*P,N*)-{P(OQuin)$_3$}RhCl(PPh$_3$)] (**1**).

Research Article
doi.org/10.1002/ejic.202300267

solutions of $P(Oquin)_3$[56] in dichloromethane (CH_2Cl_2) at low temperature (−75 °C). The reaction mixture was allowed to reach room temperature (RT), and after solvent evaporation and washing the crude product with diethyl ether, complex **1** was isolated in high yield (80 %). The product is a pale-orange solid sensitive to air and moisture. ^1H, $^{13}C\{^1H\}$, and $^{31}P\{^1H\}$ NMR spectroscopic data (including homo- and heteronuclear correlations obtained from two-dimensional spectra), elemental analysis, and LIFDI-MS (see Supporting Information, Figures S1—S8) of **1** are in accordance with the proposed structure.

The $^{31}P\{^1H\}$ NMR spectrum shows two sets of doublets of doublets (*dd*) at $\delta = 116.1$ ppm ($P(Oquin)_3$) and 49.8 ppm (PPh_3) with coupling constants of $^1J_{PRh} = 310.9$ Hz, $^2J_{PP} = 52.8$ Hz and $^1J_{PRh} = 171.1$ Hz (Figure S4, Supporting Information). The signal for $P(Oquin)_3$ is shifted to high field in contrast with the free ligand ($\delta = 130$ ppm);[55,56] while the signal for PPh_3 is downfield shifted (free PPh_3: $\delta = -5$ ppm). A comparison of the chemical shifts and coupling constants with analogous rhodium(I) complexes bearing phosphine and phosphite donors strongly suggests a *cis* configuration for **1** in solution.[62,63]

The ^1H NMR spectrum confirms the $\kappa^2(P,N)$ coordination mode of the tris(8-quinolyl)phosphite ligand (Figure S2, Supporting Information). As previously observed with the $[\kappa^2(P,N)\text{-}\{P(Oquin)_3\}PdCl_2]$ complex,[55] the resonances of $P(Oquin)_3$ in **1** appear as two separate spin systems: one for the pyridine fragment, as AMX-type ($\delta = 9.10$, 8.20, and 7.34 ppm), and one for the phenol-like ring, as ABM-type ($\delta = 7.71$, 7.54, and 7.31 ppm). The most deshielded signal ($\delta = 9.10$ ppm) corresponds to the H atom in the *ortho* position with respect to the N atom, as confirmed by 2D NMR experiments (COSY, HSQC and HMBC). At 25 °C, the resonances from the three quinoline moieties are equivalent. This spectroscopic data suggests that, in solution (CD_2Cl_2), the $P(Oquin)_3$ ligand in complex **1** is hemilabile. A similar process was previously observed for the analogous $[\kappa^2(P,N)\text{-}\{P(OQuin)_3\}PdCl_2]$ complex.[55]

Crystals of **1** suitable for single crystal X-ray analysis were obtained either from CH_2Cl_2/n-hexane or from THF/diethyl ether. The molecular structures obtained for both crystals were very similar, hence only the former one is discussed (Figure 2, see Table 1 for selected bond parameters and the Supporting Information for further details). The single crystal X-ray analysis revealed that $P(OQuin)_3$ acts as a bidentate chelate ligand toward rhodium, thus confirming the $\kappa^2(P,N)$ coordination mode of $P(OQuin)_3$ suggested by the ^1H NMR spectrum in solution. Furthermore, the *"cis"* configuration of the square planar structure indicated by the $^2J_{PP}$ coupling constants determined by solution $^{31}P\{^1H\}$ NMR spectroscopy is also present in the solid state.

The Rh–P bond lengths of **1** are significantly different, with the phosphorus atom of the phosphite unit being closer to the metal center (2.095(2) vs. 2.235(4) Å). A similar phenomenon was described by Stelzer and Montgomery for the related complexes **A** and **B** (Table 1). In these complexes the Rh–P bonds *trans* to the chlorine atoms (**A**: 2.158(2) Å; **B**: 2.106(1) Å) are noticeably shorter than those *trans* to the nitrogen donors (**A**: 2.252(3) Å; or **B**: 2.229(1) Å).[64,65] Likewise, the Rh–N1 (2.151(2) Å) and Rh–Cl1 (2.412(1) Å) distances in **1** are comparable to those reported by Stelzer (complex **A**: Rh–N 2.146(3) Å; Rh–Cl 2.429(2) Å) and Montgomery (complex **B**: Rh–N 2.162(3) Å; Rh–Cl 2.365(1) Å). Rhodium(I) complexes bearing P,N chelates known to be hemilabile in solution exhibit Rh–N bond lengths between 2.14 to 2.19 Å in the solid state.[66,67] In addition, the six-membered ring defined by Rh–N1–C1–C2–O1–P1 shows a roughly half-chair-shaped

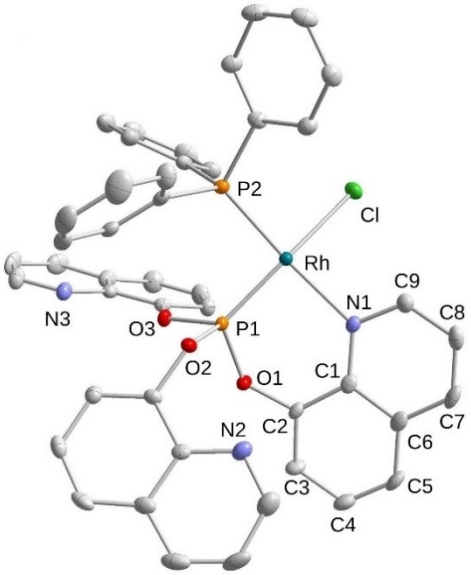

Figure 2. Molecular structure of complex $[\kappa^2(P,N)\{P(OQuin)_3\}RhCl(PPh_3)]$ (**1**). Thermal ellipsoids are drawn at 50 % probability level. Hydrogen atoms and the dichloromethane solvate molecule have been removed for clarity.

Table 1. Selected bond distances and angles for complex **1** and related compounds **A**-**C**.

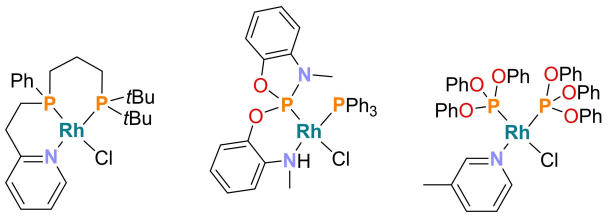

A **B** **C**

Compound	1	A[64]	B[65]	C[68]
Bond distances [Å]				
Rh–P1	2.095(2)	2.158(2)	2.106(1)	2.150(1)
Rh–P2	2.235(4)	2.252(3)	2.229(1)	2.167(1)
Rh–N1	2.151(2)	2.146(3)	2.162(3)	2.132(3)
Rh–Cl	2.412(1)	2.429(2)	2.365(1)	2.398(2)
Angles [°]				
P1–Rh–N1	90.22(5)	80.9(1)	91.36(7)	91.87(8)
P1–Rh–P2	93.16(2)	94.47(8)	94.45(3)	92.98(3)
P2–Rh–Cl1	90.57 (2)	100.14(7)	90.31(2)	89.30(3)
N1–Rh–Cl1	90.62 (5)	84.5(1)	84.00(6)	89.75(8)
P1–Rh–Cl1	160.7(2)	165.35(9)	174.78(3)	177.75(3)

Research Article
doi.org/10.1002/ejic.202300267

conformation, as seen in Montgomery's compound, **B**. The angle P1–Rh–N1 (90.22(2)°) approximates the ideal value of a square planar geometry and is close to the magnitude reported for related species (Table 1, **B** and **C**).[65,68]

The square planar molecular structure of **1** is slightly distorted as indicated by the angle between the planes P1/Rh/N1 and P2/Rh/Cl1 of 21.68(8)°. This distortion likely results from the repulsion between the $P(OQuin)_3$ and PPh_3 ligands. The two aromatic units of the coordinated quinoline moiety are slightly twisted, as indicated by the C6–C1–N1–C9 and C6–C1–C2–C3 torsion angles (−3.13(6)° and −5.85(6)° respectively). Twisting of coordinated quinoline scaffolds have also been observed in related P,N chelate complexes of rhodium and palladium.[55,69–71]

Reactivity of the Rh(I) Complex 1

NMR monitoring studies were performed to investigate the reactivity of complex **1** toward different external agents. The stability in solution of **1** in selected solvents and at different temperatures was first examined.

The stability of complex **1** in THF solution was evaluated over the course of 6 h by $^{31}P\{^1H\}$ NMR spectroscopy at 0 °C, room temperature, and at 50 °C. In every case, the complex was stable in solution, according to the NMR evidence. By contrast, in $CDCl_3$, **1** exhibits an entirely different behavior in solution (Scheme 2). $^{31}P\{^1H\}$ NMR monitoring of a dry $CDCl_3$ solution of **1** at 50 °C revealed a gradual dissociation process of the PPh_3 ligand, identified by a singlet $\delta = -5$ ppm, accompanied by coordination of a second quinoline unit of the $P(OQuin)_3$ ligand (Scheme 2a). The species formed in solution exhibits a doublet resonance at $\delta = 90.8$ ppm ($^1J_{PRh} = 161.6$ Hz) (Figure S10, Supporting Information). This phosphine ligand release and coordination of another quinoline unit reaches completion after 6 h. When **1** was dissolved in commercially available (wet) $CDCl_3$ (Scheme 2b), a different reactivity was observed. Heating this solution to 50 °C for 24 h in a J. Young NMR tube afforded several phosphorus-containing rhodium compounds. The $^{31}P\{^1H\}$ NMR spectrum of the reaction mixture shows only two sets of signals with multiplicity doublet of doublets, appearing at 1) $\delta = 69.3$ ($^1J_{PRh} = 151.0$ Hz, $^2J_{PP} = 29.5$ Hz) and $\delta = 55.5$ ($^1J_{PRh} = 146.0$ Hz, $^2J_{PP} = 30.1$ Hz) ppm, and 2) $\delta = 48.4$ ($^1J_{PRh} = 128.0$ Hz, $^2J_{PP} = 15.0$ Hz) and $\delta = 23.4$ ($^1J_{PRh} = 124.1$ Hz, $^2J_{PP} = 14.9$ Hz) ppm. The other phosphorus-containing rhodium compounds formed during this test gave rise to resonances at $\delta = 61.0$ (*d*, $^1J_{PRh} = 130.7$ Hz) and $\delta = 16.2$ (*d*, $^1J_{PRh} = 92.5$ Hz) ppm. Additionally, free PPh_3 ($\delta = -4.9$ ppm), $OPPh_3$ ($\delta = 29.7$ ppm) and a minor unidentified compound at $\delta = -15$ ppm, were also observed in the $^{31}P\{^1H\}$ NMR spectrum.

Intrigued by these results and considering that, possibly, traces of HCl formed/present in the solvent could be responsible for the behavior observed in these reactivity studies, complex **1** was deliberately treated with HCl (4.0 M 1,4-dioxane solution) in dichloromethane or THF solutions. Although this treatment afforded very unselective reaction

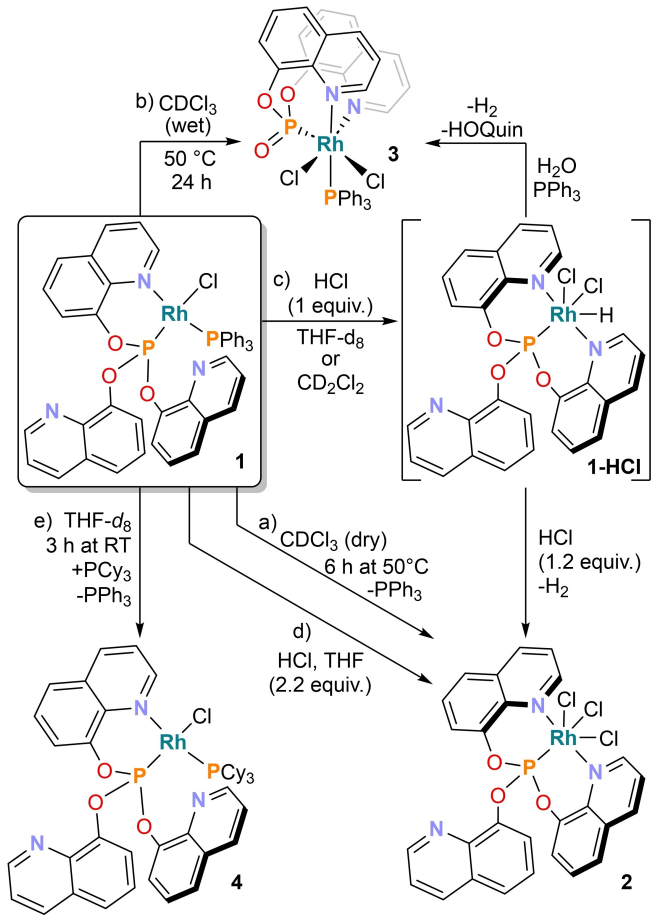

Scheme 2. Reactivity of compound **1** towards selected reagents.

mixtures and the product distribution depended on the solvent, in general, the reactions furnished similar findings in $^{31}P\{^1H\}$ NMR: the species at $\delta = 90.8$ ppm and the two sets of doublets of doublets described above. In turn, the ^1H NMR spectrum showed a hydridic species at $\delta = -15.8$ ppm (ddd, $^1J_{HRh} = 33.8$ Hz, $^2J_{HP} = 16.7$ Hz, $^2J_{HP} = 16.5$ Hz). All attempts to isolate and characterize this hydridic species were unsuccessful. However, its formation was reproducibly confirmed by several independent NMR tests. Considering this, the *in situ* formed hydride species was individually reacted with further HCl and H_2O and the reactions monitored by NMR spectroscopy. By treating the formed rhodium hydride with HCl, the doublets of doublets signals observed in $^{31}P\{^1H\}$ NMR at $\delta = 69.3$ and $\delta = 55.5$ ppm disappeared, whereas the intensity of the doublet at $\delta = 90.8$ ppm increased. This change in the $^{31}P\{^1H\}$ NMR spectrum was accompanied by the disappearance of the hydridic signal in the ^1H NMR spectrum. Moreover, addition of water to the mixture of complex **1** and HCl also causes the disappearance of the hydride signal (^1H NMR) along with an increase in the intensity of the signals at $\delta = 48.4$ and $\delta = 23.4$ ppm. Despite the lack of selectivity seen in these reactions, these observations pointed altogether toward the formation of a Rh(III) hydride complex, **1-HCl** (Scheme 2c) which is further transformed in the presence of additional

Research Article
doi.org/10.1002/ejic.202300267

amounts of acid or water to two different Rh(III) species, assigned as complexes **2** and **3**, respectively, on Scheme 2. Gratifyingly, crystals suitable for X-ray diffraction analysis, corresponding to what we assigned as compound **3**, were obtained from the $CDCl_3$ solution in the same NMR tube, and the molecular structure of **3** is shown in Figure 3 (selected bond lengths and angles in the caption figure). In complex **3** a $[OP(OQuin)_2]^-$ scaffold coordinates the Rh center in a *fac*-κ^3(*N,P,N*) mode with its phosphorus atom *cis* to the triphenylphosphine and *cis* to one chloride. The rhodium atom is in a slightly distorted octahedral geometry. The Rh–Cl1 bond is comparatively long (2.489(2) Å) likely due to the strong bonding between Rh–P1, as expected for an anionic phosphorus species. Likewise, the bond Rh–P2 (PPh_3, 2.333(4) Å) is elongated with respect to the structure **1**, which might be due to a stronger σ-donation from the quinoline moiety in *trans* position (*trans* influence).

The weakened Rh–P2 bond in complex **3** can be a useful reactive position for further applications, *e.g.* ligand substitution (*trans* effect) or catalysis. Also, for catalytic applications, the variable denticity of the ligand $[OP(OQuin)_2]^-$ could be important to stabilize reactive intermediates with lower or higher electron count and/or coordination number than that in **3**.

Unfortunately, in the case of complex **2** all attempts to grow crystals of sufficient quality for crystallographic characterization have been unsuccessful so far, and the shown structure is only proposed based on the collective NMR data obtained. **2** has been then assigned as a rhodium(III) complex, resulting from the oxidative addition of HCl to **1**, followed by subsequent protonolysis due to the presence of further amounts of HCl. Complex **2** can also be more cleanly accessed by treating a THF solution of **1** with 2.2 equivalents of HCl (Scheme 2d). In turn, and although clear evidence of the operating mechanism for the formation of species **3** is not available, we propose that its occurrence might be related to an unobserved rhodium-hydroxy-dichloride species, the putative complex [κ^3(*P,N,N*)-{$P(OQuin)_3$}$RhCl_2(OH)$], which might form by hydrolysis of hydride **1-HCl**, accompanied by elimination of a 8-hydroxyquinoline unit from the $P(OQuin)_3$ ligand in the presence of PPh_3.

A simple ligand substitution reaction was also examined. Complex **1** reacts with 1.1 equiv. of PCy_3 at room temperature yielding the related species **4** (Scheme 2e). The reaction mixture was monitored by $^{31}P\{^1H\}$ NMR and full conversion was achieved after 3 hours. The $^{31}P\{^1H\}$ NMR spectrum of the reaction mixture exhibits two new sets of doublets, free PPh_3 ($\delta = -4.5$ ppm) and $OPPh_3$ ($\delta = 24.2$ ppm) as depicted in Figure S13 in the Supporting Information.

Compound **4** gives rise to two doublets of doublets at $\delta =$ 115.7 ($^1J_{PRh} = 334.6$ Hz, $^2J_{PP} = 52.4$ Hz,$P(OQuin)_3$) and 54.1 ($^1J_{PRh} = 162.1$ Hz, $^2J_{PP} = 52.4$ Hz, PCy_3) ppm (see Figure S15, Supporting Information). Like for **1**, the ^{31}P NMR signal for $P(OQuin)_3$ is upfield shifted, while the resonance for PCy_3 is downfield shifted with respect to the corresponding resonances of the free ligands. Overall, the chemical shift values and coupling constants of **4** are analogous to the ones observed for its precursor **1**. Again, the spectroscopic evidence strongly suggests a *cis* configuration in solution.

Yellow crystals of complex **4** were isolated from a saturated acetonitrile/diethyl ether solution at −30 °C and characterized by X-ray crystallography as a diethyl ether solvate. The crystallographically determined molecular structure is shown in Figure 4, with selected bond lengths and angles in the caption figure. The X-ray diffraction analysis of complex **4** shows that, as demonstrated for **1**, the ligand $P(OQuin)_3$ binds the metal center as a κ^2(*P,N*) chelate, creating a *cis* spatial configuration between both phosphorus ligands. The other

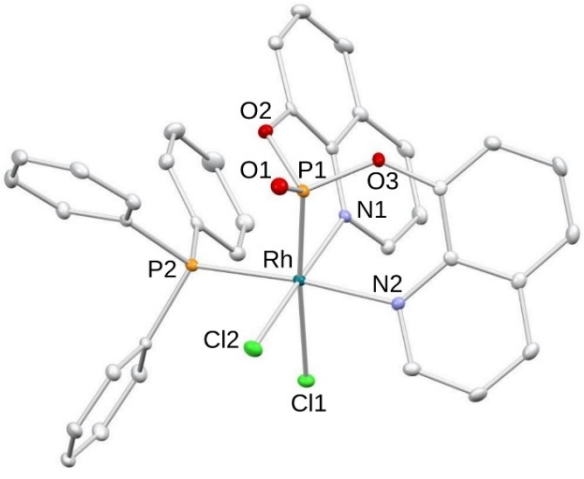

Figure 3. Molecular structure of complex [κ^3(*P,N,N*){$OP(OQuin)_2$}$RhCl_2(PPh_3)$], **3**. Thermal ellipsoids are drawn at 50% probability level. Hydrogen atoms have been removed for clarity. Selected bond lengths (Å) and angles (°) for complex **3**: Rh–P1 2.186(2), Rh–P2 2.333(4), Rh–Cl1 2.489(2), Rh–Cl2 2.325(6), Rh–N1 2.122(5), Rh–N2 2.145(6), P1–O1 1.474(4), P1–O2 1.631(2), P1–O3 1.626(6), P1–Rh–N1 84.25 (5), P1–Rh–N2 86.87 (2), P1–Rh–P2 98.47 (2), P2–Rh–N1 93.24 (5), P2–Rh–N2 174.49(2), Cl1–Rh–Cl2 88.41(2), N1–Rh–N2 88.60(2).

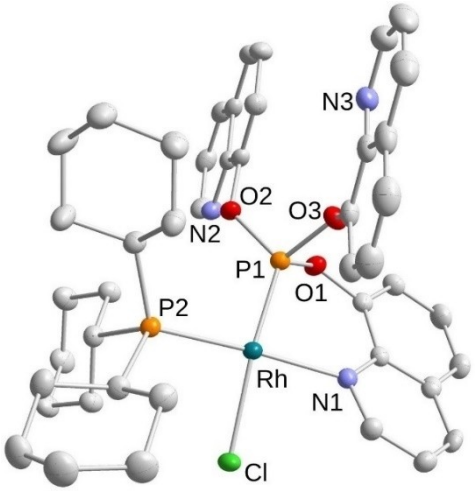

Figure 4. Molecular structure of the complex [κ^2(*P,N*)-{$P(OQuin)_3$}$RhCl(PCy_3)$], **4**. Thermal ellipsoids are drawn at 50% probability level. Hydrogen atoms and the diethyl ether solvate molecule have been removed for clarity. Selected bond lengths (Å) and angles (°) for complex **4**: Rh–P1 2.1035(5), Rh–P2 2.2765(5), Rh–Cl1 2.3849(5), Rh–N1 2.1760(18), P1–O1 1.6190(15), P1–O2 1.5993(15), P1–O3 1.6358(16), P1–Rh–P2 98.67(2), P1–Rh–N1 85.15(5), P1–Rh–Cl 166.04(2), P2–Rh–Cl 90.134(19), N1–Rh–Cl 86.56(5).

Research Article
doi.org/10.1002/ejic.202300267

two quinoline units are oriented away from the metal center. The complex exhibits a slightly distorted square planar geometry, since the chelate (plane P1/Rh/N1) is not co-planar with the chlorine and phosphorus atoms (plane P2/Rh/Cl1). The deviation from co-planarity between the planes P1/Rh/N1 and P2/Rh/Cl1 is 11.5(2) degrees.

The Rh-$P_{P(OQuin)3}$ bond distances in both complex **4** and **1** are identical within experimental error [Rh–P1(**4**) = 2.1035(5) Å vs. Rh–P1(**1**) = 2.095(2) Å], whereas the Rh-P_{PR3} (P_{PR3} = P2) and Rh–N1 bond distances are slightly longer in **4** [Rh–P2 = 2.2765(5) Å; Rh–N1 = 2.1760(18) Å], in comparison to those in **1** (see Table 1). By contrast, the Rh–Cl1 (2.383(2) Å) bond in **4** is slightly shorter than in **1**. The elongation of the Rh-P_{PR3} bond length is a consequence of the steric hindrance exerted by the encumbering PCy_3 ligand. Accordingly, the most important structural differences between **1** and **4** are seen in the bond angles. Since PCy_3 is bulkier than PPh_3, the P1-Rh-N1 (85.15(5)°) bite angle is shorter than in **1** and the P1–Rh–P2 (98.67(2)°) angle deviates considerably from 90°.

With the purpose of determining whether the coordination of an additional quinoline scaffold from $P(OQuin)_3$ was possible within the coordination sphere of **1**, the complex was reacted with chloride scavengers, such as $NaPF_6$ or NH_4PF_6. However, the reactions were unsuccessful, either at room temperature or at 50 °C, even for prolonged periods of time. The only reactivity observed in these cases was the formation of **3** as well as additional phosphorus-containing compounds generated by decomposition of complex **1**.

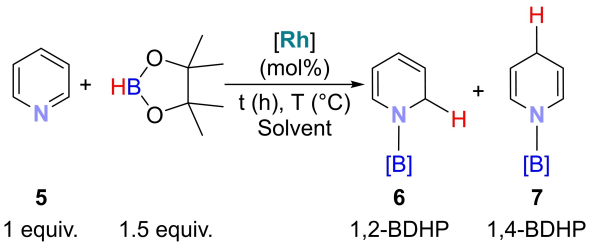

Scheme 3. Hydroboration of pyridine (Py) to N-borylated-dihydropyridine (BDHP) promoted by the Rh(I) complex **1**.

Regioselective 1,2-Hydroboration of Pyridines and Quinolines Catalyzed by 1

The regioselective hydroboration of pyridine (**5**) with pinacolborane to yield *N*-borylated-1,2-dihydropyridine (1,2-BDHP, **6**) was used as a model reaction (Scheme 3) to investigate the properties of **1** in hydroboration catalysis. The reduction of pyridine (**5**) by **1** as (pre)catalyst in C_6H_6 at 80 °C produces BDHPs in a selective manner (> 99% after 24 h; entry 4, Table 2). Under the studied conditions other Rh-based catalysts, such as $[(cod)RhCl]_2$, $[Cp^*RhCl_2]_2$ or $[(Ph_3P)_3RhCl]$, furnished the desired BDHP products in only minor yields, along with significant amounts of side products (entries 1–3, Table 2). Unlike the other Rh complexes, **1** seems to be regioselective toward the 1,2-hydroboration of Py. In the absence of catalyst (blank run) no conversion was observed (entry 11), thus confirming the catalytic nature of the transformation.

As shown in Table 2, the hydroboration proceeds selectively with a catalyst loading of complex **1** lower than 1.0 mol%. The formation of unidentified side-products is promoted when the amount of catalyst exceeds 1 mol% (entries 5–6), while catalyst loadings below 0.25 mol% lead to a significant yield drop, although the selectivity toward the desired 1,2-product increases (entries 4, 7 and 8 vs. Entries 9–10).

A systematic screening of solvents, reaction temperature and relative ratio of the different reaction components (Table S3–S6, Supporting Information) gave the following

Table 2. Screening of catalysts for the HB of Py.[a]

Entry	Rh Catalyst	Catalyst loading [mol%]	Conversion [%][b,c]	DHP [%][c]	Ratio **6**:**7**	Side Products [%][c]
1	$[(cod)RhCl]_2$	0.5	60	15	0:100	45
2	$[Cp^*RhCl_2]_2$	0.5	42	13	16:84	29
3	$[(Ph_3P)_3RhCl]$	1.0	78	9	0:100	69
4	**1**	1.0	55	55	71:29	–
5	**1**	3.0	80	62	52:48	18
6	**1**	2.0	74	67	62:38	7
7	**1**	0.75	47	47	74:26	–
8	**1**	0.5	44	44	77:23	–
9	**1**	0.25	29	29	87:13	–
10	**1**	0.1	17	17	87:13	–
11	–	–	0	0	–	–

[a] Conditions: Catalyst (as indicated), Py (11.8 mg, 150 μmol, 0.25 M) and HBpin (28.8 mg, 225 μmol; ratio [Py]:[HBpin] = 1:1.5), stirred in 0.6 mL of C_6H_6 at 80 °C for 24 h. [b] Conversion determined by ^1H NMR as consumption of Py adding 1,3,5-trimethoxybenzene (2.8 mg, 16.67 μmol) as standard after completion of the reaction. [c] Average of three individual reactions.

Research Article
doi.org/10.1002/ejic.202300267

optimized reaction conditions: [**5**] = 0.75 mol/L, 1.5 equiv. HBpin, 0.75 mol% [Rh], 18 h, 70 °C and toluene as solvent. Subsequently, a screening of different pyridines **5b**–**5g** and **5j**–**5p** quinolines was performed (Table 3). The reaction of HBpin with 4-*tert*butylpyridine (**5b**) the electron deficient 4-trifluoromethylpyridine (**5c**) and the electron-rich 4-methoxypyridine (**5d**) proceeded effectively to give the corresponding 1,2-hydroboration products in moderate to high yields and excellent selectivity. The electron-rich 3-picoline (**5g**) gave the 1,2-hydroboration product **6g** with quantitative yield and high regioselectivity (94%). In turn, 4-(dimethylamino)pyridine (**5e**) and 3-bromopyridine (**5f**) were converted to the corresponding *N*-boryl-1,2-dihydropyridines **6e** and **6f** only in 12 to 16% yield, although with good regioselectivity (> 66%). 2-Substituted pyridines (**5h**–**5i**), on the contrary, were not reduced under these conditions. It is noteworthy that the formation of 1,4-DHP compounds was not detected in most of these examples.

Table 3. Scope of the catalytic hydroboration of *N*-heteroarenes.[a–c]

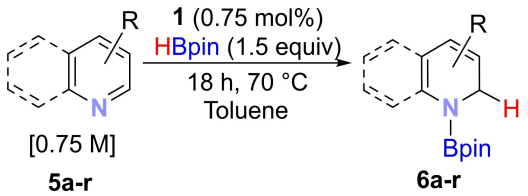

Pyridines

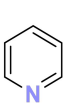
5a 84 [70:30]

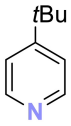

5b 51 (40) [99:1]

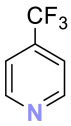

5c 93 (86) [99:1]

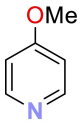

5d 95 (88) [99:1]

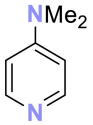

5e 12 [99:1]

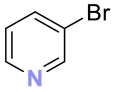

5f 16 [66:33]

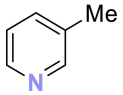

5g > 99 (81) [94:6]

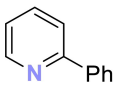

5h 0

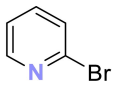

5i 0

Quinolines[d,e]

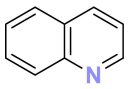
5j 85 (80) [99:1]

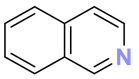
5k > 95 (87) [99:1]

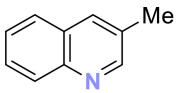

5l > 95 (90) [99:1]

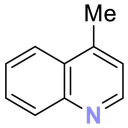

5m 63 (60) [99:1]

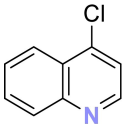

5n 70 [81:19]

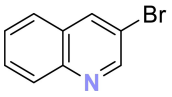

5o 56 (43) [99:1]

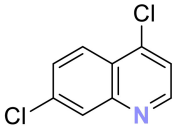

5p 60 (52) [99:1]

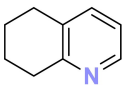
5q < 5

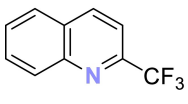

5r 0

[a] Conditions: Py or Quin (150 µmol, 0.75 M), HBpin (28.8 mg, 225 µmol, 1.5 equiv.) and [Rh] (1.12 µmol, 0.75 mol%), were stirred in 0.2 mL of toluene at 70 °C for 18 h. [b] Conversion determined by ^{1}H NMR as consumption of the corresponding substrate using 1,3,5-trimethoxybenzene (2.8 mg, 16.67 µmol) as standard after reaction. Values in parentheses (%) correspond to isolated yields. Values between brackets correspond to 1,2:1,4 ratio. [c] Average of three individual reactions. [d] HBpin (24.0 mg, 187 µmol, 1.25 equiv.). [e] 12 h.

For quinolines, the hydroboration proceeded even better than with pyridines. The developed system tolerates a variety of substrates with both electron-donating and electron-withdrawing substituents and furnished the *N*-boryl-1,2-dihydroquinoline (1,2-BDHQ) products with excellent regioselectivities (99%) for most of the substrates. Quinolines **5j**–**5l** afforded the corresponding desired products in good-to-excellent yields (> 85 %). Moderate yields of the corresponding 1,2-BDHQ were obtained with 4-methylquinoline (63%). Likewise, quinolines possessing electron-withdrawing halogen atoms (Cl, and Br) at the C3 or C4 position proceeded also well, affording 1,2-BDHQ with moderate to good yields (**5n** and **5o**, up to 70%). For the quinoline **5p**, substituted at C4 and C7 by a Cl atom, the formation of the corresponding 1,2-BDHQ compound proceeds in moderate yields (**5p**, 60%). The reduction of 5,6,7,8-tetrahydroquinoline (**5q**) or 2-trifluoromethylquinoline (**5r**) was not achieved under these reaction conditions. Similar to the case of the 2-substituted pyridine substrates (**5h**–**5i**), we attribute the lack of reactivity of **5r** to steric hindrance.

The results presented here enrich the chemistry already reported by us for the P(OQuin)$_3$ scaffold both in terms of the coordination chemistry and catalytic applications. With this, the ability of such phosphite to act as a multidentate (hemilabile) ligand for 4d transition metals is underlined and the potential to extend this chemistry to other metal ions seems feasible. The demonstrated ability of complex **1** to engage in ligand dissociation and ligand exchange processes can be exploited in future studies to access species with tunable properties for, e.g., catalytic applications.

Indeed, promising preliminary results have already been obtained with Ru(II), which will be published elsewhere. It is anticipated that the experience gathered from the coordination chemistry studies towards Pd, Rh and eventually Ru will serve as starting point to explore the chelating properties of P(OQuin)$_3$ toward the more earth abundant 3d analogues, Ni, Co and Fe. The applicability of the variable denticity of P(OQuin)$_3$ in transition-metal-catalyzed transformations is under further investigation in our groups.

Conclusions

The ability of P(OQuin)$_3$ to coordinate a Rh(I) center as a chelate ligand was demonstrated through the isolation of compounds [κ^2(*P*,*N*)-{P(OQuin)$_3$}RhCl(PR$_3$)] [R=Ph (**1**), Cy (**4**)].

The crystallographic characterization confirmed that both complexes have a distorted square planar structure and exhibit a *cis* configuration of the phosphorus ligands, which is also evident from multinuclear solution NMR data. The reactivity and stability of complex **1** toward selected reagents confirmed that this complex can be chemically transformed through ligand dissociation/exchange and oxidation. Complex **1** catalyzed the 1,2-hydroboration of pyridines and quinolines in high yield and excellent selectivity, under comparatively mild conditions (70 °C, 18 h, 1.5 equiv. of HBpin, 0.75 mol% of **1**, toluene). Turnover numbers of up to 130 were reached and almost eight molecules of the substrate were converted per molecule of catalyst in one hour for the model substrate pyridine. The described protocol tolerates a variety of substrates with both electron-donating and electron-withdrawing substituents and produces 1,2-hydroborated pyridines and quinolines (1,2-BDHP and 1,2-BDHQ) with high regioselectivities (> 95 %).

We have, therefore, demonstrated that $P(OQuin)_3$ is a versatile ligand that binds 4d metals in a variety of coordination modes and can serve as a platform for challenging catalytic transformations.

Experimental Section

General Information. A full description of the general experimental methods, characterization data of **1**–**4**,**6a**–**6q**, as well as the preparation and purification of starting materials for the catalytic studies and the procedure for the optimization of the catalytic system can be found in the Supporting Information. The synthesis of $P(OQuin)_3$ was carried out following our reported protocol.[56]

Deposition Numbers 2259166 (for **1**), 2259168 (for **3**), and 2259167 (for **4**) contain the supplementary crystallographic data for this paper. These data are provided free of charge by the joint Cambridge Crystallographic Data Centre and Fachinformationszentrum Karlsruhe Access Structures service.

Acknowledgements

Dr. Rafael E. Rodríguez-Lugo (R. E. R.-L.) thanks the Alexander von Humboldt Foundation for financial support through a Georg Forster Research Fellowship for Experienced Researchers. Dr. Vanessa R. Landaeta thanks Universidad Simón Bolívar (Decanato de Investigación y Desarrollo, DID-USB) and R. E. R.-L. thanks Instituto Venezolano de Investigaciones Científicas (IVIC) for the support received for their scientific activities. Financial support by the International PhD Program at University of Regensburg (iPUR) and German Academic Exchange Service (DAAD scholarship to Miguel A. Chacón-Terán) is gratefully acknowledged. Open Access funding enabled and organized by Projekt DEAL.

Conflict of Interests

The authors declare no conflict of interest.

Data Availability Statement

The data that support the findings of this study are available in the supplementary material of this article.

Keywords: Chelates · Hydroboration · Phosphites · Reaction mechanisms · Rhodium

[1] S. P. Roche, J. A. Porco Jr, *Angew. Chem. Int. Ed.* **2011**, *50*, 4068–4093.
[2] N. Edraki, A. R. Mehdipour, M. Khoshneviszadeh, R. Miri, *Drug Discovery Today* **2009**, *14*, 1058–1066.
[3] R. Lavilla, *J. Chem. Soc. Perkin Trans. 1* **2002**, 1141–1156.
[4] D. M. Stout, A. I. Meyers, *Chem. Rev.* **1982**, *82*, 223–243.
[5] S. Park, *ChemCatChem* **2020**, *12*, 3170–3185.
[6] V. K. Sharma, S. K. Singh, *RSC Adv.* **2017**, *7*, 2682–2732.
[7] D. Tejedor, L. Cotos, G. Méndez-Abt, F. García-Tellado, *J. Org. Chem.* **2014**, *79*, 10655–10661.
[8] F. W. Fowler, *J. Org. Chem.* **1972**, *37*, 1321–1323.
[9] R. A. Sulzbach, *J. Organomet. Chem.* **1970**, *24*, 307–314.
[10] D.-S. Wang, Q.-A. Chen, S.-M. Lu, Y.-G. Zhou, *Chem. Rev.* **2012**, *112*, 2557–2590.
[11] Y.-G. Zhou, *Acc. Chem. Res.* **2007**, *40*, 1357–1366.
[12] Y. Ji, G.-S. Feng, M.-W. Chen, L. Shi, H. Du, Y.-G. Zhou, *Org. Chem. Front.* **2017**, *4*, 1125–1129.
[13] L. Hao, J. F. Harrod, A.-M. Lebuis, Y. Mu, R. Shu, E. Samuel, H.-G. Woo, *Angew. Chem. Int. Ed.* **1998**, *37*, 3126–3129.
[14] J. F. Harrod, R. Shu, H.-G. Woo, E. Samuel, *Can. J. Chem.* **2001**, *79*, 1075–1085.
[15] S.-H. Lee, D. V Gutsulyak, G. I. Nikonov, *Organometallics* **2013**, *32*, 4457–4464.
[16] D. V Gutsulyak, A. Van der Est, G. I. Nikonov, *Angew. Chem. Int. Ed.* **2011**, *50*, 1384–1387.
[17] C. D. F. Königs, H. F. T. Klare, M. Oestreich, *Angew. Chem. Int. Ed.* **2013**, *52*, 10076–10079.
[18] N. C. Cook, J. E. Lyons, *J. Am. Chem. Soc.* **1966**, *88*, 3396–3403.
[19] K. Osakada, *Angew. Chem. Int. Ed.* **2011**, *50*, 3845–3846.
[20] D. Behera, S. Thiyagarajan, P. K. Anjalikrishna, C. H. Suresh, C. Gunanathan, *ACS Catal.* **2021**, *11*, 5885–5893.
[21] R. K. Sahoo, N. Sarkar, S. Nembenna, *Inorg. Chem.* **2023**, *62*, 304–317.
[22] J. L. Lortie, T. Dudding, B. M. Gabidullin, G. I. Nikonov, *ACS Catal.* **2017**, *7*, 8454–8459.
[23] K. Oshima, T. Ohmura, M. Suginome, *J. Am. Chem. Soc.* **2011**, *133*, 7324–7327.
[24] Kevin. Burgess, M. J. Ohlmeyer, *Chem. Rev.* **1991**, *91*, 1179–1191.
[25] I. Beletskaya, A. Pelter, *Tetrahedron* **1997**, *53*, 4957–5026.
[26] C. M. Crudden, D. Edwards, *Eur. J. Org. Chem.* **2003**, 4695–4712.
[27] A.-M. Carroll, T. P. O'Sullivan, P. J. Guiry, *Adv. Synth. Catal.* **2005**, *347*, 609–631.
[28] A. S. Dudnik, V. L. Weidner, A. Motta, M. Delferro, T. J. Marks, *Nat. Chem.* **2014**, *6*, 1100–1107.
[29] K. Oshima, T. Ohmura, M. Suginome, *J. Am. Chem. Soc.* **2012**, *134*, 3699–3702.
[30] M. Arrowsmith, M. S. Hill, T. Hadlington, G. Kociok-Köhn, C. Weetman, *Organometallics* **2011**, *30*, 5556–5559.
[31] X. Liu, B. Li, X. Hua, D. Cui, *Org. Lett.* **2020**, *22*, 4960–4965.
[32] T. Liu, J. He, Y. Zhang, *Org. Chem. Front.* **2019**, *6*, 2749–2755.
[33] S. R. Tamang, A. Singh, D. K. Unruh, M. Findlater, *ACS Catal.* **2018**, *8*, 6186–6191.
[34] P. Ji, X. Feng, S. S. Veroneau, Y. Song, W. Lin, *J. Am. Chem. Soc.* **2017**, *139*, 15600–15603.
[35] A. Kaithal, B. Chatterjee, C. Gunanathan, *Org. Lett.* **2016**, *18*, 3402–3405.
[36] P. Ji, T. Sawano, Z. Lin, A. Urban, D. Boures, W. Lin, *J. Am. Chem. Soc.* **2016**, *138*, 14860–14863.
[37] F. Zhang, H. Song, X. Zhuang, C. H. Tung, W. Wang, *J. Am. Chem. Soc.* **2017**, *139*, 17775–17778.
[38] H. Liu, M. Khononov, M. S. Eisen, *ACS Catal.* **2018**, *8*, 3673–3677.
[39] J. Intemann, M. Lutz, S. Harder, *Organometallics* **2014**, *33*, 5722–5729.
[40] C. Hu, J. Zhang, H. Yang, L. Guo, C. Cui, *Inorg. Chem.* **2021**, *60*, 14038–14046.
[41] M. Rauch, S. Ruccolo, G. Parkin, *J. Am. Chem. Soc.* **2017**, *139*, 13264–13267.

[42] H. C. Yu, S. M. Islam, N. P. Mankad, *ACS Appl. Mater. Interfaces* **2020**, *10*, 3670–3675.
[43] E. De Leon, F. Gonzalez, P. Bauskar, S. Gonzalez-Eymard, D. De Los Santos, M. M. Shoshani, *Organometallics* **2023**, *42*, 435–440.
[44] X. Fan, J. Zheng, Z. H. Li, H. Wang, *J. Am. Chem. Soc.* **2015**, *137*, 4916–4919.
[45] E. N. Keyzer, S. S. Kang, S. Hanf, D. S. Wright, *Chem. Commun.* **2017**, *53*, 9434–9437.
[46] N. Gandhamsetty, S. Park, S. Chang, *J. Am. Chem. Soc.* **2015**, *137*, 15176–15184.
[47] N. Gandhamsetty, S. Joung, S.-W. Park, S. Park, S. Chang, *J. Am. Chem. Soc.* **2014**, *136*, 16780–16783.
[48] Z. Y. Yang, H. Luo, M. Zhang, X. C. Wang, *ACS Catal.* **2021**, *11*, 10824–10829.
[49] B. Rao, C. C. Chong, R. Kinjo, *J. Am. Chem. Soc.* **2018**, *140*, 652–656.
[50] T. Hynes, E. N. Welsh, R. McDonald, M. J. Ferguson, A. W. H. Speed, *Organometallics* **2018**, *37*, 841–844.
[51] H. Yang, L. Zhang, F.-Y. Zhou, L. Jiao, *Chem. Sci.* **2020**, *11*, 742–747.
[52] A. Das, T. K. Panda, *ChemCatChem* **2023**, *15*, e202201011.
[53] J. Jeong, J. Heo, D. Kim, S. Chang, *ACS Catal.* **2020**, *10*, 5023–5029.
[54] N. Kumar Meher, P. Kumar Verma, K. Geetharani, *Org. Lett.* **2023**, *25*, 87–92.
[55] R. E. Rodríguez-Lugo, M. A. Chacón-Terán, S. De León, M. Vogt, A. J. Rosenthal, V. R. Landaeta, *Dalton Trans.* **2018**, *47*, 2061–2072.
[56] M. A. Chacón-Terán, R. E. Rodríguez-Lugo, R. Wolf, V. R. Landaeta, *Eur. J. Inorg. Chem.* **2019**, 4336–4344.
[57] V. R. Landaeta, R. E. Rodríguez-Lugo, *J. Mol. Catal. A* **2017**, *426*, 316–325.
[58] P. Braunstein, F. Naud, *Angew. Chem. Int. Ed.* **2001**, *40*, 680–699.
[59] M. P. Carroll, P. J. Guiry, *Chem. Soc. Rev.* **2014**, *43*, 819–833.
[60] P. J. Guiry, C. P. Saunders, *Adv. Synth. Catal.* **2004**, *346*, 497–537.
[61] M. Zhang, Z. Liu, W. Zhao, *Angew. Chem. Int. Ed.* **2023**, *62*, e202215455.
[62] N. Sakai, S. Mano, K. Nozaki, H. Takaya, *J. Am. Chem. Soc.* **1993**, *115*, 7033–7034.
[63] I. Choinopoulos, I. Papageorgiou, S. Coco, E. Simandiras, S. Koinis, *Polyhedron* **2012**, *45*, 255–261.
[64] A. Heßler, J. Fischer, S. Kucken, O. Stelzer, *Chem. Ber.* **1994**, *127*, 481–488.
[65] H. K. Carroll, F. G. L. Parlane, N. Reich, B. J. Jelier, C. D. Montgomery, *Inorg. Chim. Acta* **2017**, *465*, 78–83.
[66] L. J. Hounjet, R. McDonald, M. J. Ferguson, M. Cowie, *Inorg. Chem.* **2011**, *50*, 5361–5378.
[67] L. J. Hounjet, M. Bierenstiel, M. J. Ferguson, R. McDonald, M. Cowie, *Dalton Trans.* **2009**, 4213–4226.
[68] A. M. Trzeciak, J. J. Ziółkowski, T. Lis, *J. Organomet. Chem.* **1991**, *419*, 391–398.
[69] D. Drommi, F. Faraone, G. Franciò, D. Belletti, C. Graiff, A. Tiripicchio, *Organometallics* **2002**, *21*, 761–764.
[70] B. Crociani, S. Antonaroli, M. Burattini, F. Benetollo, A. Scrivanti, M. Bertoldini, *J. Organomet. Chem.* **2008**, *693*, 3932–3938.
[71] E. Cook, J. D. Masuda, A. Xia, *Can. J. Chem.* **2009**, *88*, 99–103.

Manuscript received: May 8, 2023
Revised manuscript received: July 31, 2023
Accepted manuscript online: August 6, 2023
Version of record online: ■■, ■■

RESEARCH ARTICLE

A rhodium(I) complex of the tris(8-quinolinyl)phosphite ligand, P-(OQuin)$_3$, enables the 1,2-regioselective hydroboration of pyridines and quinolines. P(OQuin)$_3$ coordinates to rhodium as a bidentate P,N chelate ligand. Reactivity studies of **1** showed that the PPh_3 ligand can be substituted intermolecularly by PCy_3 and intramolecularly by a second unit 8-quinolyl of P(OQuin)$_3$.

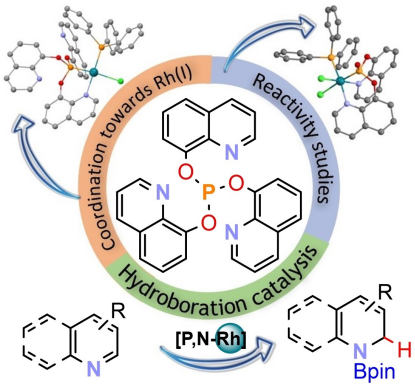

Dr. M. A. Chacón-Terán, Dr. V. R. Landaeta, Prof. Dr. R. Wolf*, Dr. R. E. Rodríguez-Lugo**

1 – 10

Regioselective Rhodium-Catalyzed 1,2-Hydroboration of Pyridines and Quinolines Enabled by the Tris(8-quinolinyl)phosphite Ligand